

## Updated $B_s$ -mixing constraints on new physics models for $b \rightarrow s\ell^+\ell^-$ anomalies

Luca Di Luzio,<sup>\*</sup> Matthew Kirk,<sup>†</sup> and Alexander Lenz<sup>‡</sup>

*Institute for Particle Physics Phenomenology, Department of Physics, Durham University, DH1 3LE Durham, United Kingdom*

 (Received 7 February 2018; published 25 May 2018)

Many new physics models that explain the intriguing anomalies in the  $b$ -quark flavor sector are severely constrained by  $B_s$  mixing, for which the Standard Model prediction and experiment agreed well until recently. The most recent Flavour Lattice Averaging Group (FLAG) average of lattice results for the nonperturbative matrix elements points, however, in the direction of a small discrepancy in this observable Cabibbo-Kobayashi-Maskawa (CKM). Using up-to-date inputs from standard sources such as PDG, FLAG and one of the two leading CKM fitting groups to determine  $\Delta M_s^{\text{SM}}$ , we find a severe reduction of the allowed parameter space of  $Z'$  and leptoquark models explaining the  $B$  anomalies. Remarkably, in the former case the upper bound on the  $Z'$  mass approaches dangerously close to the energy scales already probed by the LHC. We finally identify some model-building directions in order to alleviate the tension with  $B_s$  mixing.

DOI: 10.1103/PhysRevD.97.095035

### I. INTRODUCTION

Direct searches for new physics (NP) effects at the LHC have so far shown no discrepancies from the Standard Model (SM), while we have an intriguing list of deviations between experiment and theory for flavor observables. In particular  $b \rightarrow s\ell^+\ell^-$  transitions seem to be in tension with the SM expectations: branching ratios of hadronic  $b \rightarrow s\mu^+\mu^-$  decays [1–3] and the angular distributions for  $B \rightarrow K^{(*)}\mu^+\mu^-$  decay [2–11] hint at a negative, beyond the SM (BSM) contribution to  $C_9$  [12–23]. The significance of the effect is still under discussion because of the difficulty of determining the exact size of the hadronic contributions (see e.g. [24–30]). Estimates of the combined significance of all these deviations range between 3 and almost 6 standard deviations. A theoretically much cleaner observable is given by the lepton flavor universality (LFU) ratios  $R_K$  and  $R_{K^*}$  [31,32], where hadronic uncertainties drop out to a very large extent. Here again a sizeable deviation from the SM expectation is found by LHCb [33,34]. Such an effect might arise for instance from new particles coupling to  $b\bar{s}$  and  $\mu^+\mu^-$ , while leaving the  $e^+e^-$  coupling mainly unchanged (see e.g. [35–64] for an arbitrary set of papers

investigating  $Z'$  models). Any new  $b\bar{s}$  coupling immediately leads to tree-level contributions to  $B_s$  mixing, which is severely constrained by experiment. For quite some time the SM value for the mass difference  $\Delta M_s$  of neutral  $B_s$  mesons—triggering the oscillation frequency—was in perfect agreement with experiment, see e.g. [65] or [66]. Taking, however, the most recent lattice inputs, in particular the new average provided by the Flavour Lattice Averaging Group (FLAG) one gets a SM value considerably above the measurement. In this paper we investigate the drastic consequences of this new theory prediction. In Sec. II we review the SM prediction of  $B_s$  mixing, whose consequences for BSM models trying to explain the  $B$  anomalies are studied in Sec. III. We conclude in Sec. IV. In the Appendices we give further details of the SM prediction as well as a more critical discussion of the theoretical uncertainties.

### II. $B_s$ MIXING IN THE SM

The mass difference of the mass eigenstates of the neutral  $B_s$  mesons is given by

$$\Delta M_s \equiv M_H^s - M_L^s = 2|M_{12}^s|. \quad (1)$$

The calculation of the box diagrams in Fig. 1 gives the SM value for  $M_{12}^s$ , see e.g. [65] for a brief review, and one gets

$$M_{12}^s = \frac{G_F^2}{12\pi^2} \lambda_t^2 M_W^2 S_0(x_t) B f_{B_s}^2 M_{B_s} \hat{\eta}_B, \quad (2)$$

<sup>\*</sup>luca.di-luzio@durham.ac.uk

<sup>†</sup>m.j.kirk@durham.ac.uk

<sup>‡</sup>alexander.lenz@durham.ac.uk

Published by the American Physical Society under the terms of the Creative Commons Attribution 4.0 International license. Further distribution of this work must maintain attribution to the author(s) and the published article's title, journal citation, and DOI. Funded by SCOAP<sup>3</sup>.

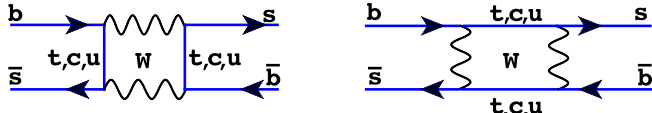


FIG. 1. SM diagrams for the transition between  $B_s$  and  $\bar{B}_s$  mesons. The contribution of internal off-shell particles is denoted by  $M_{12}^s$ .

with the Fermi constant  $G_F$ , the masses of the  $W$  boson,  $M_W$ , and of the  $B_s$  meson,  $M_{B_s}$ . Using CKM unitarity one finds only one contributing CKM structure  $\lambda_t = V_{ts}^* V_{tb}$ . The CKM elements are the only place in Eq. (2) where an imaginary part can arise. The result of the 1-loop diagrams given in Fig. 1 is denoted by the Inami-Lim function [67]  $S_0(x_t) = (\bar{m}_t(\bar{m}_t))^2/M_W^2 \approx 2.36853$ , where  $\bar{m}_t(\bar{m}_t)$  is the  $\overline{\text{MS}}$  mass [68] of the top quark. Perturbative 2-loop QCD corrections are compressed in the factor  $\hat{\eta}_B \approx 0.83798$ , they have been calculated by [69]. In the SM calculation of  $M_{12}^s$  one four-quark  $\Delta B = 2$  operator arises

$$Q = \bar{s}^\alpha \gamma_\mu (1 - \gamma_5) b^\alpha \times \bar{s}^\beta \gamma^\mu (1 - \gamma_5) b^\beta. \quad (3)$$

The hadronic matrix element of this operator is parametrized in terms of a decay constant  $f_{B_s}$  and a bag parameter  $B$ :

$$\langle Q \rangle \equiv \langle B_s^0 | Q | \bar{B}_s^0 \rangle = \frac{8}{3} M_{B_s}^2 f_{B_s}^2 B(\mu). \quad (4)$$

We also indicated the renormalization scale dependence of the bag parameter; in our analysis we take  $\mu = \bar{m}_b(\bar{m}_b)$ . Sometimes a different notation for the QCD corrections and the bag parameter is used in the literature (e.g. by FLAG: [70]),  $(\eta_B, \hat{B})$  instead of  $(\hat{\eta}_B, B)$  with

$$\hat{\eta}_B B \equiv \eta_B \hat{B} = \eta_B \alpha_s(\mu)^{-\frac{6}{23}} \left[ 1 + \frac{\alpha_s(\mu)}{4\pi} \frac{5165}{3174} \right] B, \quad (5)$$

$$\hat{B} = 1.51926B. \quad (6)$$

The parameter  $\hat{B}$  has the advantage of being renormalization scale and scheme independent. A commonly used SM prediction of  $\Delta M_s$  was given by [65,66]

$$\Delta M_s^{\text{SM}, 2011} = (17.3 \pm 2.6) \text{ ps}^{-1}, \quad (7)$$

$$\Delta M_s^{\text{SM}, 2015} = (18.3 \pm 2.7) \text{ ps}^{-1}. \quad (8)$$

Both predictions agreed very well with the experimental measurement [71]

$$\Delta M_s^{\text{Exp}} = (17.757 \pm 0.021) \text{ ps}^{-1}. \quad (9)$$

In 2016 Fermilab/MILC presented a new calculation [72], which gave considerably larger values for the non-perturbative parameter, resulting in values around  $20 \text{ ps}^{-1}$  for the mass difference [72–76] and being thus larger than experiment. An independent confirmation of these large values would of course be desirable; a first step in that direction has been done by the HQET sum rule calculation of [77] which is in agreement with Fermilab/MILC for the bag parameters.

Using the most recent numerical inputs listed in Appendix A we predict the mass difference of the neutral  $B_s$  mesons to be<sup>1</sup>

$$\Delta M_s^{\text{SM}, 2017} = (20.01 \pm 1.25) \text{ ps}^{-1}. \quad (10)$$

Here the dominant uncertainty still comes from the lattice predictions for the nonperturbative parameters  $B$  and  $f_{B_s}$ , giving a relative error of 5.8%. The uncertainty in the CKM elements contributes 2.1% to the error budget. The CKM parameters were determined assuming unitarity of the  $3 \times 3$  CKM matrix. The uncertainties due to  $m_t$ ,  $m_b$  and  $\alpha_s$  can be safely neglected at the current stage. A detailed discussion of the input parameters and the error budget is given in Appendixes A and B, respectively. The new central value for the mass difference in Eq. (10) is  $1.8\sigma$  above the experimental one given in Eq. (9). This difference has profound implications for NP models that predict sizeable positive contributions to  $B_s$  mixing. The new value for the SM prediction depends strongly on the nonperturbative input as well as the values of the CKM elements. We use the averages that are provided by the lattice community (FLAG) and by one of the two leading CKM fitting groups (CKMfitter)—see Appendix C and Appendix D for a further discussion of these inputs.

### III. $B_s$ MIXING BEYOND THE SM

To determine the allowed space for NP effects in  $B_s$  mixing we compare the experimental measurement of the mass difference with the prediction in the SM plus NP:

$$\Delta M_s^{\text{Exp}} = 2|M_{12}^{\text{SM}} + M_{12}^{\text{NP}}| = \Delta M_s^{\text{SM}} \left| 1 + \frac{M_{12}^{\text{NP}}}{M_{12}^{\text{SM}}} \right|. \quad (11)$$

For this equation we will use in the SM part the CKM elements, which have been determined assuming the validity of the SM. In the presence of BSM effects the CKM elements used in the prediction of  $M_{12}^{\text{SM}}$  could in general differ from the ones we use—see e.g. the case of a fourth chiral fermion generation [78]. In the following, we

<sup>1</sup>A more conservative determination of the SM value of the mass difference using only tree-level inputs for the CKM parameters can be found in Eq. (D10).

will assume that NP effects do not involve sizeable shifts in the CKM elements.

A simple estimate shows that the improvement of the SM prediction from Eqs. (7)–(8) to (10) can have a drastic impact on the size of the allowed BSM effects on  $B_s$  mixing. For a generic NP model we can parametrize

$$\frac{\Delta M_s^{\text{Exp}}}{\Delta M_s^{\text{SM}}} = \left| 1 + \frac{\kappa}{\Lambda_{\text{NP}}^2} \right|, \quad (12)$$

where  $\Lambda_{\text{NP}}$  denotes the mass scale of the NP mediator and  $\kappa$  is a dimensionful quantity which encodes NP couplings and the SM contribution. If  $\kappa > 0$ , which is often the case in many BSM scenarios for  $B$  anomalies considered in the literature, and since  $\Delta M_s^{\text{SM}} > \Delta M_s^{\text{Exp}}$ , the  $2\sigma$  bound on  $\Lambda_{\text{NP}}$  scales like

$$\frac{\Lambda_{\text{NP}}^{2017}}{\Lambda_{\text{NP}}^{2015}} = \sqrt{\frac{\frac{\Delta M_s^{\text{Exp}}}{(\Delta M_s^{\text{SM}} - 2\delta\Delta M_s^{\text{SM}})^{2015}} - 1}{\frac{\Delta M_s^{\text{Exp}}}{(\Delta M_s^{\text{SM}} - 2\delta\Delta M_s^{\text{SM}})^{2017}} - 1}} \simeq 5.2, \quad (13)$$

where  $\delta\Delta M_s^{\text{SM}}$  denotes the  $1\sigma$  error of the SM prediction. Hence, in models where  $\kappa > 0$ , the limit on the mass of the NP mediators is strengthened by a factor 5. On the other hand, if the tension between the SM prediction and  $\Delta M_s^{\text{Exp}}$  increases in the future, a NP contribution with  $\kappa < 0$  would be required in order to accommodate the discrepancy.

A typical example where  $\kappa > 0$  is that of a purely LH vector-current operator, which arises from the exchange of a single mediator featuring real couplings, cf. Sec. III A.<sup>2</sup> In such a case, the short-distance contribution to  $B_s$  mixing is described by the effective Lagrangian

$$\mathcal{L}_{\Delta B=2}^{\text{NP}} = -\frac{4G_F}{\sqrt{2}} (V_{tb}V_{ts}^*)^2 [C_{bs}^{LL} (\bar{s}_L\gamma_\mu b_L)^2 + \text{H.c.}], \quad (14)$$

where  $C_{bs}^{LL}$  is a Wilson coefficient to be matched with ultraviolet (UV) models, and which enters Eq. (11) as

$$\frac{\Delta M_s^{\text{Exp}}}{\Delta M_s^{\text{SM}}} = \left| 1 + \frac{C_{bs}^{LL}}{R_{\text{SM}}^{\text{loop}}} \right|, \quad (15)$$

where

$$R_{\text{SM}}^{\text{loop}} = \frac{\sqrt{2}G_F M_W^2 \hat{\eta}_B S_0(x_t)}{16\pi^2} = 1.3397 \times 10^{-3}. \quad (16)$$

In the following, we will show how the updated bound from  $\Delta M_s$  impacts the parameter space of simplified models (with  $\kappa > 0$ ) put forth for the explanation of the recent discrepancies in semileptonic  $B$ -physics data

<sup>2</sup>Similar scenarios leading to  $\kappa > 0$  were considered in 2016 by Blanke and Buras [73] in the context of CMFV models.

(Sec. III A) and then discuss some model-building directions in order to achieve  $\kappa < 0$  (Sec. III B).

### A. Impact of $B_s$ mixing on NP models for $B$ anomalies

A useful application of the refined SM prediction in Eq. (10) is in the context of the recent hints of LFU violation in semileptonic  $B$ -meson decays, both in neutral and charged currents. Focusing first on neutral current anomalies, the main observables are the LFU violating ratios  $R_{K^{(*)}} \equiv \mathcal{B}(B \rightarrow K^{(*)}\mu^+\mu^-)/\mathcal{B}(B \rightarrow K^{(*)}e^+e^-)$  [33,34], together with the angular distributions of  $B \rightarrow K^{(*)}\mu^+\mu^-$  [2–11] and the branching ratios of hadronic  $b \rightarrow s\mu^+\mu^-$  decays [1–3]. As hinted by various recent global fits [18–23], and in order to simplify a bit the discussion, we assume NP contributions only in purely LH vector currents involving muons. The generalization to different type of operators is straightforward. The effective Lagrangian for semi-leptonic  $b \rightarrow s\mu^+\mu^-$  transitions contains the terms

$$\mathcal{L}_{b \rightarrow s\mu\mu}^{\text{NP}} \supset \frac{4G_F}{\sqrt{2}} V_{tb}V_{ts}^* (\delta C_9^\mu O_9^\mu + \delta C_{10}^\mu O_{10}^\mu) + \text{H.c.}, \quad (17)$$

with

$$O_9^\mu = \frac{\alpha}{4\pi} (\bar{s}_L\gamma_\mu b_L)(\bar{\mu}\gamma^\mu\mu), \quad (18)$$

$$O_{10}^\mu = \frac{\alpha}{4\pi} (\bar{s}_L\gamma_\mu b_L)(\bar{\mu}\gamma^\mu\gamma_5\mu). \quad (19)$$

Assuming purely LH currents and real Wilson coefficients the best fit of  $R_K$  and  $R_{K^*}$  yields (from e.g. [21])  $\text{Re}(\delta C_9^\mu) = -\text{Re}(\delta C_{10}^\mu) \in [-0.81, -0.48]$  ( $[-1.00, -0.32]$ ) at  $1\sigma$  ( $2\sigma$ ). Adding also the data on  $B \rightarrow K^{(*)}\mu^+\mu^-$  angular distributions and other  $b \rightarrow s\mu^+\mu^-$  observables<sup>3</sup> improves the statistical significance of the fit, but does not necessarily imply larger deviations of  $\text{Re}(\delta C_9^\mu)$  from zero (see e.g. [20]). In the following we will stick only to the  $R_K$  and  $R_{K^*}$  observables and denote this benchmark as “ $R_{K^{(*)}}$ .”

#### 1. $Z'$

A paradigmatic NP model for explaining the  $B$  anomalies in neutral currents is that of a  $Z'$  dominantly coupled via LH currents. Here, we focus only on the part of the Lagrangian relevant for  $b \rightarrow s\mu^+\mu^-$  transitions and  $B_s$  mixing, namely

$$\mathcal{L}_{Z'} = \frac{1}{2} M_{Z'}^2 (Z'_\mu)^2 + (\lambda_{ij}^Q \bar{d}_L^i \gamma^\mu d_L^j + \lambda_{\alpha\beta}^L \bar{\ell}_L^\alpha \gamma^\mu \ell_L^\beta) Z'_\mu, \quad (20)$$

<sup>3</sup>These include for instance  $\mathcal{B}(B_s \rightarrow \mu^+\mu^-)$  which is particularly constraining in the case of pseudoscalar mediated quark transitions (see e.g. [79]).

where  $d^i$  and  $\ell^\alpha$  denote down-quark and charged-lepton mass eigenstates, and  $\lambda^{Q,L}$  are Hermitian matrices in flavor space. Of course, any full-fledged [i.e.  $SU(2)_L \times U(1)_Y$  gauge invariant and anomaly free]  $Z'$  model attempting an explanation of  $R_{K^{(*)}}$  via LH currents can be mapped into Eq. (20). After integrating out the  $Z'$  at tree level, we obtain the effective Lagrangian

$$\begin{aligned} \mathcal{L}_{Z'}^{\text{eff}} &= -\frac{1}{2M_{Z'}^2} (\lambda_{ij}^Q \bar{d}_L^i \gamma_\mu d_L^j + \lambda_{\alpha\beta}^L \bar{\ell}_L^\alpha \gamma_\mu \ell_L^\beta)^2 \\ &\supset -\frac{1}{2M_{Z'}^2} [(\lambda_{23}^Q)^2 (\bar{s}_L \gamma_\mu b_L)^2 \\ &\quad + 2\lambda_{23}^Q \lambda_{22}^L (\bar{s}_L \gamma_\mu b_L) (\bar{\mu}_L \gamma_\mu \mu_L) + \text{H.c.}]. \end{aligned} \quad (21)$$

Matching with Eqs. (17) and (14) we get

$$\delta C_9^\mu = -\delta C_{10}^\mu = -\frac{\pi}{\sqrt{2} G_F M_{Z'}^2 \alpha} \left( \frac{\lambda_{23}^Q \lambda_{22}^L}{V_{tb} V_{ts}^*} \right), \quad (22)$$

and

$$C_{bs}^{LL} = \frac{\eta^{LL}(M_{Z'})}{4\sqrt{2} G_F M_{Z'}^2} \left( \frac{\lambda_{23}^Q}{V_{tb} V_{ts}^*} \right)^2, \quad (23)$$

where  $\eta^{LL}(M_{Z'})$  encodes the running down to the bottom mass scale using NLO anomalous dimensions [80,81]. For example, for  $M_{Z'} \in [1, 10]$  TeV we find  $\eta^{LL}(M_{Z'}) \in [0.79, 0.75]$ .

Here we consider the case of a real coupling  $\lambda_{23}^Q$ , so that  $C_{bs}^{LL} > 0$  and  $\delta C_9^\mu = -\delta C_{10}^\mu$  is also real. This assumption is consistent with the fact that nearly all the groups performing global fits [12–23] (see however [82] for an exception) assumed so far real Wilson coefficients in Eq. (17) and also follows the standard approach adopted in the literature for the  $Z'$  models aiming at an explanation of the  $b \rightarrow s\mu^+\mu^-$  anomalies (for an incomplete list, see [35–64]). In fact, complex  $Z'$  couplings can arise via fermion mixing, but are subject to additional constraints from  $CP$ -violating observables (cf. Sec. III B).

The impact of the improved SM calculation of  $B_s$  mixing on the parameter space of the  $Z'$  explanation of  $R_{K^{(*)}}$  is displayed in Fig. 2, for the reference value  $\lambda_{22}^L = 1$ .<sup>4</sup> Note that the old SM determination,  $\Delta M_s^{\text{SM}, 2015}$ , allowed for  $M_{Z'}$  as heavy as  $\approx 10$  TeV in order to explain  $R_{K^{(*)}}$  at  $1\sigma$ . In contrast,  $\Delta M_s^{\text{SM}, 2017}$  implies now  $M_{Z'} \lesssim 2$  TeV. Remarkably, even for  $\lambda_{22}^L = \sqrt{4\pi}$ , which saturates the perturbative unitarity bound [85,86], we find that the updated limit from  $B_s$  mixing requires  $M_{Z'} \lesssim 8$  TeV for the  $1\sigma$  explanation of  $R_{K^{(*)}}$ . Whether a few TeV  $Z'$  is ruled out or not by direct searches at LHC depends however on the details of

<sup>4</sup>For  $m_{Z'} \lesssim 1$  TeV the coupling  $\lambda_{22}^L$  is bounded by the  $Z \rightarrow 4\mu$  measurement at LHC and by neutrino trident production [83]. See for instance Fig. 1 in [84] for a recent analysis.

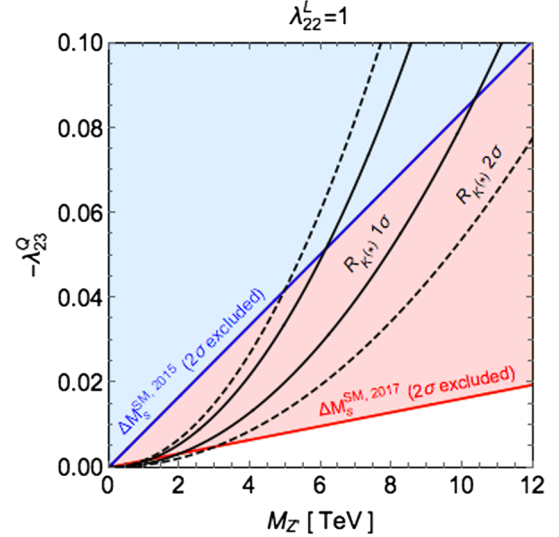


FIG. 2. Bounds from  $B_s$  mixing on the parameter space of the simplified  $Z'$  model of Eq. (20), for real  $\lambda_{23}^Q$  and  $\lambda_{22}^L = 1$ . The blue and red shaded areas correspond respectively to the  $2\sigma$  exclusions from  $\Delta M_s^{\text{SM}, 2015}$  and  $\Delta M_s^{\text{SM}, 2017}$ , while the solid (dashed) black curves encompass the  $1\sigma$  ( $2\sigma$ ) best-fit region from  $R_{K^{(*)}}$ .

the  $Z'$  model. For instance, the stringent constraints from dilepton searches [87] are tamed in models where the  $Z'$  couples mainly third generation fermions (as e.g. in [63]). This notwithstanding, the updated limit from  $B_s$  mixing cuts dramatically into the parameter space of the  $Z'$  explanation of the  $b \rightarrow s\mu^+\mu^-$  anomalies, with important implications for LHC direct searches and future colliders [88].

## 2. Leptoquarks

Another popular class of simplified models which has been proposed in order to address the  $b \rightarrow s\mu^+\mu^-$  anomalies consists in leptoquark mediators (see e.g. [89–106]). Although  $B_s$  mixing is generated at one loop [107,108],<sup>5</sup> and hence the constraints are expected to be milder compared to the  $Z'$  case, the connection with the anomalies is more direct due to the structure of the leptoquark couplings. For instance, let us consider the scalar-leptoquark  $S_3 \sim (\bar{3}, 3, 1/3)$ ,<sup>6</sup> with the Lagrangian

$$\mathcal{L}_{S_3} = -M_{S_3}^2 |S_3^a|^2 + y_{ia}^{QL} \bar{Q}^i (\epsilon \sigma^a) L^a S_3^a + \text{H.c.}, \quad (24)$$

where  $\sigma^a$  (for  $a = 1, 2, 3$ ) are Pauli matrices,  $\epsilon = i\sigma^2$ , and we employed the quark  $Q^i = (V_{ji}^* u_L^j, d_L^i)^T$  and lepton

<sup>5</sup>The scalar-leptoquark model proposed in Ref. [101] is a notable exception.

<sup>6</sup>Similar considerations apply to the vector leptoquarks  $U_1^\mu \sim (3, 1, 2/3)$  and  $U_3^\mu \sim (3, 3, 2/3)$ , which also provide a good fit for  $R_{K^{(*)}}$ . The case of massive vectors is however subtler, since the calculability of loop observables depends upon the UV completion (for a recent discussion, see e.g. [109]).

$L^\alpha = (\nu_L^\alpha \ell_L^\alpha)^T$  doublet representations ( $V$  being the CKM matrix). The contribution to the Wilson coefficients in Eq. (17) arises at tree level and reads

$$\delta C_9^\mu = -\delta C_{10}^\mu = \frac{\pi}{\sqrt{2}G_F M_{S_3}^2} \alpha \begin{pmatrix} y_{32}^{OL} y_{22}^{OL*} \\ V_{tb} V_{ts}^* \end{pmatrix}, \quad (25)$$

while that to  $B_s$  mixing in Eq. (14) is induced at one loop [110]

$$C_{bs}^{LL} = \frac{\eta^{LL}(M_{S_3})}{4\sqrt{2}G_F M_{S_3}^2} \frac{5}{64\pi^2} \left( \frac{y_{3\alpha}^{OL} y_{2\alpha}^{OL*}}{V_{tb} V_{ts}^*} \right)^2, \quad (26)$$

where the sum over the leptonic index  $\alpha = 1, 2, 3$  is understood. In order to compare the two observables we consider in Fig. 3 the case in which only the couplings  $y_{32}^{OL} y_{22}^{OL*}$  (namely those directly connected to  $R_{K^{(*)}}$ ) contribute to  $B_s$  mixing and further assume real couplings, so that we can use the results of global fits which apply to real  $\delta C_9^\mu = -\delta C_{10}^\mu$ .

The bound on  $M_{S_3}$  from  $B_s$  mixing is strengthened by a factor 5 thanks to the new determination of  $\Delta M_s$ , which yields  $M_{S_3} \lesssim 22$  TeV, in order to explain  $R_{K^{(*)}}$  at  $1\sigma$  (cf. Fig. 3). On the other hand, in flavor models predicting a hierarchical structure for the leptoquark couplings one rather expects  $y_{i3}^{OL} \gg y_{i2}^{OL}$ , so that the dominant contribution to  $\Delta M_s$  is given by  $y_{33}^{OL} y_{23}^{OL*}$ . For example,  $y_{i3}^{OL}/y_{i2}^{OL} \sim \sqrt{m_\tau/m_\mu} \approx 4$  in the partial compositeness framework of Ref. [90], so that the upper bound on  $M_{S_3}$  is strengthened by a factor  $y_{33}^{OL} y_{23}^{OL*}/y_{32}^{OL} y_{22}^{OL*} \sim 16$ . The latter can then easily approach the limits from LHC direct searches which

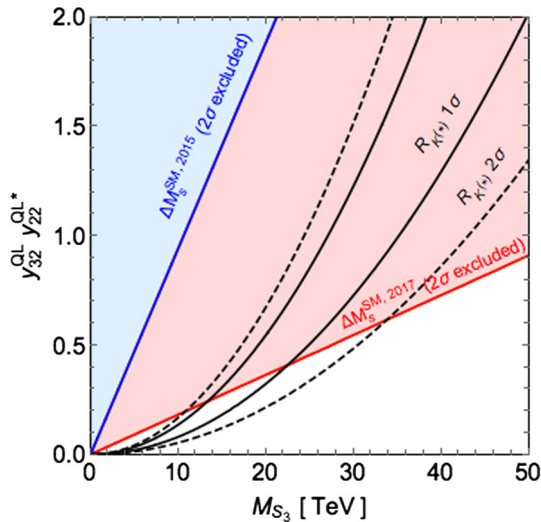


FIG. 3. Bounds from  $B_s$  mixing on the parameter space of the scalar-leptoquark model of Eq. (24), for real  $y_{32}^{OL} y_{22}^{OL*}$  couplings. Meaning of shaded areas and curves as in Fig. 2.

imply  $M_{S_3} \gtrsim 900$  GeV, e.g. for a QCD pair-produced  $S_3$  dominantly coupled to third generation fermions [111].

### 3. Combined $R_{K^{(*)}}$ and $R_{D^{(*)}}$ explanations

Another set of intriguing anomalies in  $B$ -physics data is that related to the LFU violating ratios  $R_{D^{(*)}} \equiv \mathcal{B}(B \rightarrow D^{(*)} \tau \bar{\nu})/\mathcal{B}(B \rightarrow D^{(*)} \ell \bar{\nu})$  (here,  $\ell = e, \mu$ ), which turn out to be larger than the SM [112–114]. Notably, in this case NP must compete with a tree-level SM charged current, thus requiring a sizeably larger effect compared to neutral current anomalies. The conditions under which a combined explanation of  $R_{K^{(*)}}$  and  $R_{D^{(*)}}$  can be obtained, compatibly with a plethora of other indirect constraints (as e.g. those pointed out in [115,116]), have been recently reassessed at the EFT level in Ref. [117]. Regarding  $B_s$ -mixing, dimensional analysis [see e.g. Eq. (6) in [117]] shows that models without some additional dynamical suppression (compared to semileptonic operators) are severely constrained already with the old  $\Delta M_s$  value. For instance, solutions based on a vector triplet  $V' \sim (1, 3, 0)$  [118], where  $B_s$  mixing arises at tree level, are in serious tension with data unless one invokes e.g. a percent level cancellation from extra contributions [117]. The updated value of  $\Delta M_s$  in Eq. (10) makes the tuning required to achieve that even worse. On the other hand, leptoquark solutions [e.g. the vector  $U_1^\mu \sim (3, 1, 2/3)$ ] comply better with the bound due to the fact that  $B_s$  mixing arises at one loop, but the contribution to  $\Delta M_s$  should be actually addressed in specific UV models whenever calculable [104].

### B. Model-building directions for $\Delta M_s^{\text{NP}} < 0$

Given the fact that  $\Delta M_s^{\text{SM}} > \Delta M_s^{\text{exp}}$  at about  $2\sigma$ , it is interesting to speculate about possible ways to obtain a negative NP contribution to  $\Delta M_s$ , thus relaxing the tension between the SM and the experimental measurement.

Sticking to the simplified models of Sec. III A ( $Z'$  and leptoquarks coupled only to LH currents), an obvious solution in order to achieve  $C_{bs}^{LL} < 0$  is to allow for complex couplings [cf. Eqs. (23) and (26)]. For instance, in  $Z'$  models this could happen as a consequence of fermion mixing if the  $Z'$  does not couple universally in the gauge-current basis. A similar mechanism could be at play for vector leptoquarks arising from a spontaneously broken gauge theory, while scalar-leptoquark couplings to SM fermions are in general complex even before going in the mass basis.

Extra phases in the couplings are constrained by  $CP$ -violating observables, that we discuss in turn. In order to quantify the allowed parameter space for a generic, complex coefficient  $C_{bs}^{LL}$  in Eq. (14), we parametrize NP effects in  $B_s$  mixing via

$$\frac{M_{12}^{\text{SM+NP}}}{M_{12}^{\text{SM}}} \equiv |\Delta| e^{i\phi_\Delta}, \quad (27)$$

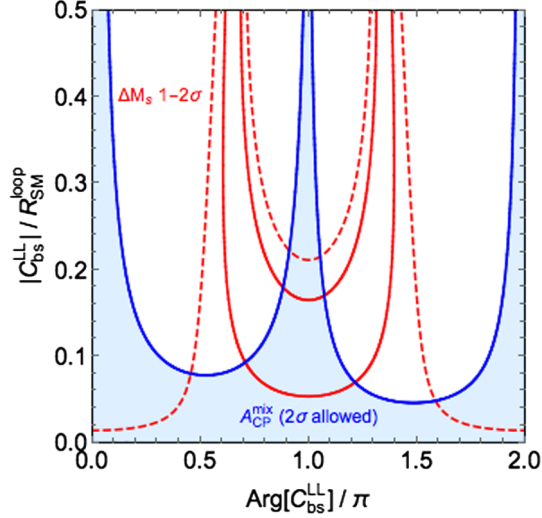


FIG. 4. Combined constraints on the complex Wilson coefficient  $C_{bs}^{LL}$ . The blue shaded area is the  $2\sigma$  allowed region from  $A_{CP}^{\text{mix}}$ , while the solid (dashed) red curves enclose the  $1\sigma$  ( $2\sigma$ ) regions from  $\Delta M_s^{\text{SM}, 2017}$ .

where

$$|\Delta| = \left| 1 + \frac{C_{bs}^{LL}}{R_{SM}^{\text{loop}}} \right|, \quad \phi_{\Delta} = \text{Arg} \left( 1 + \frac{C_{bs}^{LL}}{R_{SM}^{\text{loop}}} \right). \quad (28)$$

The former is constrained by  $\Delta M_s^{\text{Exp}} / \Delta M_s^{\text{SM}} = |\Delta|$ , while the latter by the mixing-induced  $CP$  asymmetry [65, 119]<sup>7</sup>

$$A_{CP}^{\text{mix}}(B_s \rightarrow J/\psi\phi) = \sin(\phi_{\Delta} - 2\beta_s), \quad (29)$$

where  $A_{CP}^{\text{mix}} = -0.021 \pm 0.031$  [71],  $\beta_s = 0.01852 \pm 0.00032$  [120], and we neglected penguin contributions [65]. The combined  $2\sigma$  constraints on the Wilson coefficient  $C_{bs}^{LL}$  are displayed in Fig. 4.

For  $\text{Arg}(C_{bs}^{LL})=0$  we recover the  $2\sigma$  bound  $|C_{bs}^{LL}|/R_{SM}^{\text{loop}} \lesssim 0.014$ , which basically corresponds to the case discussed in Sec. III A where we assumed a nearly real  $C_{bs}^{LL}$  (up to a small imaginary part due to  $V_{ts}$ ). On the other hand, a nonzero phase of  $C_{bs}^{LL}$  allows us to relax the bound from  $\Delta M_s$ , or even accommodate  $\Delta M_s$  at  $1\sigma$  (region between the two solid red curves in Fig. 4), compatibly with the  $2\sigma$  allowed region from  $A_{CP}^{\text{mix}}$  (blue shaded area in Fig. 4). For  $\text{Arg}(C_{bs}^{LL}) \approx \pi$  values of  $|C_{bs}^{LL}|/R_{SM}^{\text{loop}}$  as high as 0.21 are allowed at  $2\sigma$ , relaxing the bound on the modulus of the Wilson coefficient by a factor 15 with respect to the  $\text{Arg}(C_{bs}^{LL})=0$  case. Note, however, that the limit  $\text{Arg}(C_{bs}^{LL}) = \pi$  corresponds to a nearly imaginary  $\delta C_9^{\mu} = -\delta C_{10}^{\mu}$  which would presumably spoil the fit of  $R_{K^{(*)}}$ , since

<sup>7</sup>The semileptonic  $CP$  asymmetries for flavor-specific decays,  $a_{\text{sl}}^s$ , do not pose serious constraints since the experimental errors are still too large [65].

the interference with the SM contribution would be strongly suppressed. Nevertheless, it would be interesting to perform a global fit of  $R_{K^{(*)}}$ , together with  $\Delta M_s$  and  $A_{CP}^{\text{mix}}$  while allowing for nonzero values of the phase, in order to see whether a better agreement with the data can be obtained. Nonzero weak phases can potentially reveal themselves also via their contribution to triple product  $CP$  asymmetries in  $B \rightarrow K^{(*)}\mu^+\mu^-$  angular distributions [82]. This is however beyond the scope of the present paper and we leave it for a future work.

An alternative way to achieve a negative contribution for  $\Delta M_s^{\text{NP}}$  is to go beyond the simplified models of Sec. III A and contemplate generalized chirality structures. Let us consider for definiteness the case of a  $Z'$  coupled both to left handed (LH) and (right handed) RH down-quark currents

$$\mathcal{L}_{Z'} \supset \frac{1}{2} M_{Z'}^2 (Z'_{\mu})^2 + (\lambda_{ij}^O \bar{d}_i^{\mu} \gamma^{\mu} d_L^j + \lambda_{ij}^d \bar{d}_i^{\mu} \gamma^{\mu} d_R^j) Z'_{\mu}. \quad (30)$$

Upon integrating out the  $Z'$  one obtains

$$\begin{aligned} \mathcal{L}_{Z'}^{\text{eff}} \supset & -\frac{1}{2M_{Z'}^2} [(\lambda_{23}^O)^2 (\bar{s}_L \gamma_{\mu} b_L)^2 + (\lambda_{23}^d)^2 (\bar{s}_R \gamma_{\mu} b_R)^2 \\ & + 2\lambda_{23}^O \lambda_{23}^d (\bar{s}_L \gamma_{\mu} b_L)(\bar{s}_R \gamma_{\mu} b_R) + \text{H.c.}]. \end{aligned} \quad (31)$$

The LR vector operator can clearly have any sign, even for real couplings. Moreover, since it gets strongly enhanced by renormalization-group effects compared to left-left and right-right vector operators [121], it can easily dominate the contribution to  $\Delta M_s^{\text{NP}}$ . Note, however, that  $\lambda_{23}^d$  contributes to  $R_{K^{(*)}}$  via RH quark currents whose presence is disfavored by global fits, since they break the approximate relation  $R_K \approx R_{K^*}$  that is observed experimentally (see e.g. [22]). Hence, also in this case, a careful study would be required in order to assess the simultaneous explanation of  $R_{K^{(*)}}$  and  $\Delta M_s$ .

## IV. CONCLUSIONS

In this paper, we have updated the SM prediction for the  $B_s$ -mixing observable  $\Delta M_s$  [Eq. (10)] using the most recent values for the input parameters, in particular new results from the lattice averaging group FLAG. Our update shifts the central value of the SM theory prediction upwards and away from experiment by 13%, while reducing the theory uncertainty compared to the previous SM determination by a factor of 2. This implies a  $1.8\sigma$  discrepancy from the SM.

We further discussed an important application of the  $\Delta M_s$  update for NP models aimed at explaining the recent anomalies in semileptonic  $B_s$  decays. The latter typically predict a positive shift in the NP contribution to  $\Delta M_s$ , thus making the discrepancy with respect to the experimental value even worse. As a generic result we have shown that, whenever the NP contribution to  $\Delta M_s$  is positive, the limit

on the mass of the NP mediators that must be invoked to explain any of the anomalies is strengthened by a factor of 5 (for a given size of couplings) compared to using the 2015 SM calculation for  $\Delta M_s$ .

In particular, we considered two representative examples of NP models featuring purely LH current and real couplings—that of a  $Z'$  with the minimal couplings needed to explain  $R_{K^{(*)}}$  anomalies, and a scalar  $[SU(2)_L$  triplet] leptoquark model. For the  $Z'$  case we get an upper bound on the  $Z'$  mass of 2 TeV (for unit  $Z'$  coupling to muons, cf. Fig. 2), an energy scale that is already probed by direct searches at LHC. On the other hand, the bounds on leptoquark models from  $B_s$  mixing are generically milder, being the latter loop suppressed. For instance, taking only the contribution of the couplings needed to fit  $R_{K^{(*)}}$  for the evaluation of  $\Delta M_s$  we find that the upper bound on the scalar-leptoquark mass is brought down to about 20 TeV (cf. Fig. 3). This limit gets however strengthened in flavor models predicting a hierarchical structure of the leptoquark couplings to SM fermions and can easily approach the region probed by the LHC. Trying in addition to solve the deviations in  $R_{D^{(*)}}$  implies very severe bounds from  $B_s$  mixing as well, since the overall scale of NP must be lowered compared to the case of only neutral current anomalies.

Given the current status of a higher theory value for  $\Delta M_s$  compared to experiment, we also have looked at possible ways in which NP can provide a *negative* contribution that lessens the tension. A nonzero phase in the NP couplings is one such way, and we have shown how extra constraints from the  $CP$ -violating observable  $A_{CP}^{\text{mix}}$  in  $B_s \rightarrow J/\psi\phi$  decays cuts out parameter space where otherwise a significant NP contribution could be present. However, a large phase can potentially worsen the fit for  $R_{K^{(*)}}$ —here a global combined fit of  $\Delta M_s$ ,  $A_{CP}^{\text{mix}}$  and  $R_{K^{(*)}}$  seems to be an important next step. Another possibility is to consider NP models with a generalized chirality structure. In particular,  $\Delta B = 2$  LR vector operators, which are renormalisation-group enhanced, can accommodate any sign for  $\Delta M_s^{\text{NP}}$ , even for real couplings. Large contributions from RH currents are however disfavoured by the  $R_{K^{(*)}}$  fit, hence also here a more careful analysis is needed.

Finally, a confirmation of our results, by further lattice groups confirming the large FNAL/MILC results for the four quark matrix elements, as well as a definite solution of the  $V_{cb}$  puzzle, would give further confidence in the extraordinary strength of the bounds presented in this paper.

## ACKNOWLEDGMENTS

We thank Sébastien Descotes-Genon for providing the unpublished *tree-level only* CKM values obtained by CKMfitter, Tomomi Ishikawa and Andreas Jüttner for advice on lattice inputs and Marco Nardecchia for helpful

feedback on the BSM section. This work was supported by the STFC through the IPPP grant.

## APPENDIX A: NUMERICAL INPUT FOR THEORY PREDICTIONS

We use the following input for our numerical evaluations. The values in Table I are taken from the PDG [122], from nonrelativistic sum rules (NRSR) [123,124], from the CKMfitter group (web update of [120]—similar values can be taken from the UTfit group [125]) and the nonperturbative parameters from FLAG (web update of [70]). For  $\alpha_s$  we use RunDec [126] with 5-loop accuracy [127–131], running from  $M_Z$  down to the bottom mass scale. At the low scale we use 2-loop accuracy to determine  $\Lambda^{(5)}$ .

## APPENDIX B: ERROR BUDGET OF THE THEORY PREDICTIONS

In this appendix we compare the error budget of our new SM prediction for  $\Delta M_s^{\text{SM}}$  with the ones given in 2015 by [65], in 2011 by [66] and 2006 by [119]. The numbers are given in Table II.

We observe a considerable improvement in accuracy and a sizeable shift compared to the 2015 prediction, mostly stemming from the new lattice results for  $f_{B_s}\sqrt{B}$ , which still is responsible for the largest error contribution of about 6%. The next important uncertainty is the accuracy of the CKM element  $V_{cb}$ , which contributes about 2% to the error budget. If one gives up the assumption of the unitarity of the  $3 \times 3$  CKM matrix, the uncertainty can go up. The uncertainties due to the remaining parameters play a less important role. All in all we are left with an overall uncertainty of about 6%, which

TABLE I. List of input parameters needed for an update of the theory prediction of different mixing observables.

Parameter	Value	Reference
$M_W$	80.385(15) GeV	PDG 2017
$G_F$	$1.1663787(6)10^{-5}$ GeV <sup>-2</sup>	PDG 2017
$\hbar$	$6.582119514(40)10^{-25}$ GeV s	PDG 2017
$M_{B_s}$	5.36689(19) GeV	PDG 2017
$m_t$	173.1(0.6) GeV	PDG 2017
$\bar{m}_t(\bar{m}_t)$	165.65(57) GeV	own evaluation
$\bar{m}_b(\bar{m}_b)$	4.203(25) GeV	NRSR
$\alpha_s(M_Z)$	0.1181(11)	PDG 2017
$\alpha_s(\bar{m}_b)$	0.2246(21)	own evaluation
$\Lambda^{(5)}$	0.2259(68) GeV	own evaluation
$V_{us}$	$0.22508^{+0.00030}_{-0.00028}$	CKMfitter
$V_{cb}$	$0.04181^{+0.00028}_{-0.00060}$	CKMfitter
$ V_{ub}/V_{cb} $	0.0889(14)	CKMfitter
$\gamma_{\text{CKM}}$	$1.141^{+0.017}_{-0.020}$	CKMfitter
$f_{B_s}\sqrt{B}$	274(8) MeV	FLAG

TABLE II. List of the individual contributions to the theoretical error of the mass difference  $\Delta M_s$  within the SM and comparison with the values obtained in [65,66], and [119]. In the last row, the errors are summed in quadrature.

$\Delta M_s^{\text{SM}}$	This work	ABL 2015 [65]	LN 2011 [66]	LN 2006 [119]
Central Value	20.01 ps <sup>-1</sup>	18.3 ps <sup>-1</sup>	17.3 ps <sup>-1</sup>	19.3 ps <sup>-1</sup>
$\delta(f_{B_s}\sqrt{B})$	5.8%	13.9%	13.5%	34.1%
$\delta(V_{cb})$	2.1%	4.9%	3.4%	4.9%
$\delta(m_t)$	0.7%	0.7%	1.1%	1.8%
$\delta(\alpha_s)$	0.1%	0.1%	0.4%	2.0%
$\delta(\gamma_{\text{CKM}})$	0.1%	0.1%	0.3%	1.0%
$\delta( V_{ub}/V_{cb} )$	<0.1%	0.1%	0.2%	0.5%
$\delta(\bar{m}_b)$	<0.1%	<0.1%	0.1%	...
$\sum \delta$	6.2%	14.8%	14.0%	34.6%

has to be compared to the experimental uncertainty of about 1 per mille.

### APPENDIX C: NONPERTURBATIVE INPUTS

As a word of caution we present here a wider range of nonperturbative determinations of the matrix elements of the four-quark operators including also the corresponding predictions for the mass differences, see Table III.

HPQCD presented in 2014 preliminary results for  $N_f = 2 + 1$  in [132] and for our numerical estimate in Table III we had to read off the numbers from Fig. 3 in their proceedings [132]. When finalized, this new calculation will supersede the 2006 [137] and 2009 [134] values. The ETMC  $N_f = 2$  number stems from 2013 [133], it is obtained with only two active flavors in the lattice simulation. The Fermilab/MILC  $N_f = 2 + 1$  number stems from 2016 [72] and it supersedes the 2011 value [139]. This precise value is currently dominating the FLAG average. The numerical effect of these new inputs on mixing observables was e.g. studied in [74]. The previous

TABLE III. List of predictions for the nonperturbative parameter  $f_{B_s}\sqrt{B}$  and the corresponding SM prediction for  $\Delta M_s$ . The current FLAG average is dominated by the FERMILAB/MILC value from 2016.

Source	$f_{B_s}\sqrt{B}$	$\Delta M_s^{\text{SM}}$
HPQCD14 [132]	(247 ± 12) MeV	(16.2 ± 1.7) ps <sup>-1</sup>
ETMC13 [133]	(262 ± 10) MeV	(18.3 ± 1.5) ps <sup>-1</sup>
HPQCD09 [134] = FLAG13 [135]	(266 ± 18) MeV	(18.9 ± 2.6) ps <sup>-1</sup>
<b>FLAG17 [70]</b>	<b>(274 ± 8) MeV</b>	<b>(20.01 ± 1.25) ps<sup>-1</sup></b>
Fermilab16 [72]	(274.6 ± 8.8) MeV	(20.1 ± 1.5) ps <sup>-1</sup>
HQET-SR [77,136]	(278 <sup>+28</sup> <sub>-24</sub> ) MeV	(20.6 <sup>+4.4</sup> <sub>-3.4</sub> ) ps <sup>-1</sup>
HPQCD06 [137]	(281 ± 20) MeV	(21.0 ± 3.0) ps <sup>-1</sup>
RBC/UKQCD14 [138]	(290 ± 20) MeV	(22.4 ± 3.4) ps <sup>-1</sup>
Fermilab11 [139]	(291 ± 18) MeV	(22.6 ± 2.8) ps <sup>-1</sup>

FLAG average from 2013 [135] was considerably lower. There is also a large  $N_f = 2 + 1$  value from RBC-UKQCD presented at LATTICE 2015 (update of [138]). However, this number is obtained in the static limit and currently missing  $1/m_b$  corrections are expected to be very sizeable [140]. The HQET sum rules estimate for the Bag parameter [77] can also be combined with the decay constant from lattice.

Here clearly a convergence of these determinations, in particular an independent confirmation of the Fermilab/MILC result which is currently dominating the FLAG average, would be very desirable.

### APPENDIX D: CKM DEPENDENCE

The second most important input parameter for the prediction of  $\Delta M_s$  is the CKM parameter  $V_{cb}$ . There is a longstanding discrepancy between the inclusive determination and values obtained from studying exclusive  $B$  decays, see [122]. Recent studies found, however, that the low exclusive value might actually be a problem originating in the use of a certain form factor parametrization in the experimental analysis.<sup>8</sup> Using the Boyd, Grinstein, Lebed (BGL) parametrization one finds values that lie considerably closer to the inclusive one, see [143–146]. Currently, there are various determinations of  $V_{cb}$  available:

$$V_{cb}^{\text{Inclusive}} = 0.04219 \pm 0.00078 \quad [71], \quad (\text{D1})$$

$$V_{cb}^{B \rightarrow D} = 0.03918 \pm 0.00094 \pm 0.00031 \quad [71], \quad (\text{D2})$$

$$V_{cb}^{B \rightarrow D^*, \text{CLN}} = 0.03871 \pm 0.00047 \pm 0.00059 \quad [71], \quad (\text{D3})$$

$$V_{cb}^{B \rightarrow D^*, \text{BGL}} = 0.0419^{+0.0020}_{-0.0019} \quad [142]. \quad (\text{D4})$$

In Fig. 5 we plot the dependence of the SM prediction of  $\Delta M_s$  on  $V_{cb}$ , and show the regions predicted by the above inclusive and exclusive determinations. We use the CKMfitter result for  $V_{cb}$  (see Table I) for our new SM prediction of  $\Delta M_s$  [see Eq. (10) and the (upper) horizontal dashed line denoted with “SM”], the corresponding error band is shown in orange. The predictions obtained by using the inclusive value of  $V_{cb}$  only is given by the blue region. For completeness we show also the regions obtained by using the exclusive extractions of  $V_{cb}$ . The disfavored CLN values result in much lower values for the mass difference (hatched areas), while the BGL value agrees well with the inclusive region, albeit with a higher uncertainty. The experimental value of  $\Delta M_s$  is shown by the (lower) horizontal dashed line denoted with “Exp.”

<sup>8</sup>The form factor models are denoted by CLN [141] and BGL [142]. Traditionally experiments were using CLN. It turned out, however, that CLN might underestimate some uncertainties.

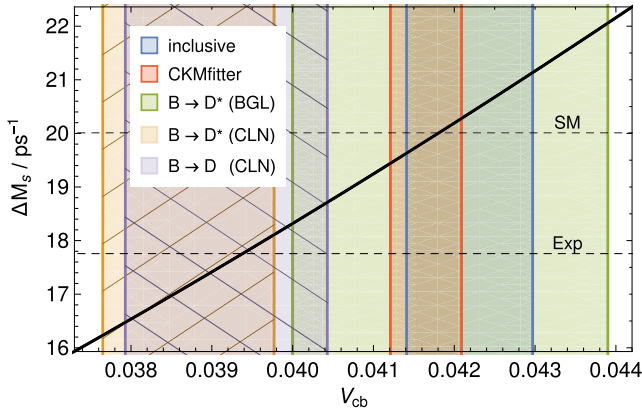


FIG. 5. Dependence of the SM prediction for  $\Delta M_s$  from the value of the CKM element  $V_{cb}$ . See text for details.

The preference for the inclusive determination agrees also with the value obtained from the CKM fit (which we use in our SM estimate), as well as with the fit value that is found if the direct measurements of  $V_{cb}$  are not included in the fit

$$V_{cb}^{\text{CKM-fitter (no direct)}} = 0.04235_{-0.00069}^{+0.00074} \quad [120]. \quad (\text{D5})$$

We also note that the CKMfitter determinations take into account loop-mediated processes, where potentially NP can arise. Taking only tree-level inputs, they find [147]

$$V_{us} = 0.22520_{-0.00038}^{+0.00012}, \quad (\text{D6})$$

$$V_{cb} = 0.04175_{-0.00172}^{+0.00033}, \quad (\text{D7})$$

$$|V_{ub}/V_{cb}| = 0.092_{-0.005}^{+0.004}, \quad (\text{D8})$$

$$\gamma_{\text{CKM}} = 1.223_{-0.030}^{+0.017}, \quad (\text{D9})$$

and using these inputs we find

$$\Delta M_s^{\text{SM, 2017(tree)}} = (19.9 \pm 1.5) \text{ ps}^{-1}, \quad (\text{D10})$$

which shows an overall consistency with the prediction in Eq. (10).

- 
- [1] R. Aaij *et al.* (LHCb Collaboration), *J. High Energy Phys.* **06** (2014) 133.
  - [2] R. Aaij *et al.* (LHCb Collaboration), *J. High Energy Phys.* **09** (2015) 179.
  - [3] V. Khachatryan *et al.* (CMS Collaboration), *Phys. Lett. B* **753**, 424 (2016).
  - [4] J. P. Lees *et al.* (BABAR Collaboration), *Phys. Rev. D* **93**, 052015 (2016).
  - [5] J. T. Wei *et al.* (Belle Collaboration), *Phys. Rev. Lett.* **103**, 171801 (2009).
  - [6] T. Aaltonen *et al.* (CDF Collaboration), *Phys. Rev. Lett.* **108**, 081807 (2012).
  - [7] R. Aaij *et al.* (LHCb Collaboration), *J. High Energy Phys.* **02** (2016) 104.
  - [8] A. Abdesselam *et al.* (Belle Collaboration), arXiv: 1604.04042.
  - [9] S. Wehle *et al.* (Belle Collaboration), *Phys. Rev. Lett.* **118**, 111801 (2017).
  - [10] M. Aaboud *et al.* (ATLAS Collaboration), arXiv: 1805.04000.
  - [11] A. M. Sirunyan *et al.* (CMS Collaboration), *Phys. Lett. B* **781**, 517 (2018).
  - [12] S. Descotes-Genon, J. Matias, and J. Virto, *Phys. Rev. D* **88**, 074002 (2013).
  - [13] F. Beaujean, C. Bobeth, and D. van Dyk, *Eur. Phys. J. C* **74**, 2897 (2014); **74**, 3179(E) (2014).
  - [14] W. Altmannshofer and D. M. Straub, *Eur. Phys. J. C* **75**, 382 (2015).
  - [15] S. Descotes-Genon, L. Hofer, J. Matias, and J. Virto, *J. High Energy Phys.* **06** (2016) 092.
  - [16] T. Hurth, F. Mahmoudi, and S. Neshatpour, *Nucl. Phys.* **B909**, 737 (2016).
  - [17] W. Altmannshofer, C. Niehoff, P. Stangl, and D. M. Straub, *Eur. Phys. J. C* **77**, 377 (2017).
  - [18] M. Ciuchini, A. M. Coutinho, M. Fedele, E. Franco, A. Paul, L. Silvestrini, and M. Valli, *Eur. Phys. J. C* **77**, 688 (2017).
  - [19] L.-S. Geng, B. Grinstein, S. Jger, J. Martin Camalich, X.-L. Ren, and R.-X. Shi, *Phys. Rev. D* **96**, 093006 (2017).
  - [20] B. Capdevila, A. Crivellin, S. Descotes-Genon, J. Matias, and J. Virto, *J. High Energy Phys.* **01** (2018) 093.
  - [21] W. Altmannshofer, P. Stangl, and D. M. Straub, *Phys. Rev. D* **96**, 055008 (2017).
  - [22] G. D'Amico, M. Nardecchia, P. Panci, F. Sannino, A. Strumia, R. Torre, and A. Urbano, *J. High Energy Phys.* **09** (2017) 010.
  - [23] A. K. Alok, B. Bhattacharya, A. Datta, D. Kumar, J. Kumar, and D. London, *Phys. Rev. D* **96**, 095009 (2017).
  - [24] S. Jger and J. Martin Camalich, *J. High Energy Phys.* **05** (2013) 043.
  - [25] S. Jger and J. Martin Camalich, *Phys. Rev. D* **93**, 014028 (2016).
  - [26] S. Descotes-Genon, L. Hofer, J. Matias, and J. Virto, *J. High Energy Phys.* **12** (2014) 125.
  - [27] M. Ciuchini, M. Fedele, E. Franco, S. Mishima, A. Paul, L. Silvestrini, and M. Valli, *J. High Energy Phys.* **06** (2016) 116.
  - [28] V. G. Chobanova, T. Hurth, F. Mahmoudi, D. Martinez Santos, and S. Neshatpour, *J. High Energy Phys.* **07** (2017) 025.

- [29] B. Capdevila, S. Descotes-Genon, L. Hofer, and J. Matias, *J. High Energy Phys.* **04** (2017) 016.
- [30] C. Bobeth, M. Chrzaszcz, D. van Dyk, and J. Virto, [arXiv:1707.07305](https://arxiv.org/abs/1707.07305).
- [31] G. Hiller and F. Kruger, *Phys. Rev. D* **69**, 074020 (2004).
- [32] M. Bordone, G. Isidori, and A. Pattori, *Eur. Phys. J. C* **76**, 440 (2016).
- [33] R. Aaij *et al.* (LHCb Collaboration), *Phys. Rev. Lett.* **113**, 151601 (2014).
- [34] R. Aaij *et al.* (LHCb Collaboration), *J. High Energy Phys.* **08** (2017) 055.
- [35] A. J. Buras and J. Girrbach, *J. High Energy Phys.* **12** (2013) 009.
- [36] R. Gauld, F. Goertz, and U. Haisch, *J. High Energy Phys.* **01** (2014) 069.
- [37] A. J. Buras, F. De Fazio, and J. Girrbach, *J. High Energy Phys.* **02** (2014) 112.
- [38] W. Altmannshofer, S. Gori, M. Pospelov, and I. Yavin, *Phys. Rev. D* **89**, 095033 (2014).
- [39] A. Crivellin, G. D'Ambrosio, and J. Heeck, *Phys. Rev. Lett.* **114**, 151801 (2015).
- [40] A. Crivellin, G. D'Ambrosio, and J. Heeck, *Phys. Rev. D* **91**, 075006 (2015).
- [41] A. Celis, J. Fuentes-Martin, M. Jung, and H. Serodio, *Phys. Rev. D* **92**, 015007 (2015).
- [42] G. Belanger, C. Delaunay, and S. Westhoff, *Phys. Rev. D* **92**, 055021 (2015).
- [43] A. Falkowski, M. Nardecchia, and R. Ziegler, *J. High Energy Phys.* **11** (2015) 173.
- [44] A. Carmona and F. Goertz, *Phys. Rev. Lett.* **116**, 251801 (2016).
- [45] B. Allanach, F. S. Queiroz, A. Strumia, and S. Sun, *Phys. Rev. D* **93**, 055045 (2016); **95**, 119902(E) (2017).
- [46] C.-W. Chiang, X.-G. He, and G. Valencia, *Phys. Rev. D* **93**, 074003 (2016).
- [47] S. M. Boucenna, A. Celis, J. Fuentes-Martin, A. Vicente, and J. Virto, *Phys. Lett. B* **760**, 214 (2016).
- [48] E. Megias, G. Panico, O. Pujolas, and M. Quiros, *J. High Energy Phys.* **09** (2016) 118.
- [49] S. M. Boucenna, A. Celis, J. Fuentes-Martin, A. Vicente, and J. Virto, *J. High Energy Phys.* **12** (2016) 059.
- [50] W. Altmannshofer, S. Gori, S. Profumo, and F. S. Queiroz, *J. High Energy Phys.* **12** (2016) 106.
- [51] A. Crivellin, J. Fuentes-Martin, A. Greljo, and G. Isidori, *Phys. Lett. B* **766**, 77 (2017).
- [52] I. Garcia Garcia, *J. High Energy Phys.* **03** (2017) 040.
- [53] D. Bhatia, S. Chakraborty, and A. Dighe, *J. High Energy Phys.* **03** (2017) 117.
- [54] J. M. Cline, J. M. Cornell, D. London, and R. Watanabe, *Phys. Rev. D* **95**, 095015 (2017).
- [55] S. Baek, *Phys. Lett. B* **781**, 376 (2018).
- [56] J. M. Cline and J. Martin Camalich, *Phys. Rev. D* **96**, 055036 (2017).
- [57] S. Di Chiara, A. Fowlie, S. Fraser, C. Marzo, L. Marzola, M. Raidal, and C. Spethmann, *Nucl. Phys.* **B923**, 245 (2017).
- [58] J. F. Kamenik, Y. Soreq, and J. Zupan, *Phys. Rev. D* **97**, 035002 (2018).
- [59] P. Ko, Y. Omura, Y. Shigekami, and C. Yu, *Phys. Rev. D* **95**, 115040 (2017).
- [60] P. Ko, T. Nomura, and H. Okada, *Phys. Rev. D* **95**, 111701 (2017).
- [61] R. Alonso, P. Cox, C. Han, and T. T. Yanagida, *Phys. Rev. D* **96**, 071701 (2017).
- [62] J. Ellis, M. Fairbairn, and P. Tunney, *Eur. Phys. J. C* **78**, 238 (2018).
- [63] R. Alonso, P. Cox, C. Han, and T. T. Yanagida, *Phys. Lett. B* **774**, 643 (2017).
- [64] A. Carmona and F. Goertz, [arXiv:1712.02536](https://arxiv.org/abs/1712.02536).
- [65] M. Artuso, G. Borisso, and A. Lenz, *Rev. Mod. Phys.* **88**, 045002 (2016).
- [66] A. Lenz and U. Nierste, [arXiv:1102.4274](https://arxiv.org/abs/1102.4274).
- [67] T. Inami and C. S. Lim, *Prog. Theor. Phys.* **65**, 297 (1981); **65**, 1772(E) (1981).
- [68] W. A. Bardeen, A. J. Buras, D. W. Duke, and T. Muta, *Phys. Rev. D* **18**, 3998 (1978).
- [69] A. J. Buras, M. Jamin, and P. H. Weisz, *Nucl. Phys.* **B347**, 491 (1990).
- [70] S. Aoki *et al.*, *Eur. Phys. J. C* **77**, 112 (2017).
- [71] Y. Amhis *et al.*, *Eur. Phys. J. C* **77**, 895 (2017).
- [72] A. Bazavov *et al.* (Fermilab Lattice, MILC Collaboration), *Phys. Rev. D* **93**, 113016 (2016).
- [73] M. Blanke and A. J. Buras, *Eur. Phys. J. C* **76**, 197 (2016).
- [74] T. Jubb, M. Kirk, A. Lenz, and G. Tetlalmatzi-Xolocotzi, *Nucl. Phys.* **B915**, 431 (2017).
- [75] A. J. Buras and F. De Fazio, *J. High Energy Phys.* **08** (2016) 115.
- [76] W. Altmannshofer, S. Gori, D. J. Robinson, and D. Tuckler, *J. High Energy Phys.* **03** (2018) 129.
- [77] M. Kirk, A. Lenz, and T. Rauh, *J. High Energy Phys.* **12** (2017) 068.
- [78] M. Bobrowski, A. Lenz, J. Riedl, and J. Rohrwild, *Phys. Rev. D* **79**, 113006 (2009).
- [79] E. Golowich, J. Hewett, S. Pakvasa, A. A. Petrov, and G. K. Yeghiyan, *Phys. Rev. D* **83**, 114017 (2011).
- [80] M. Ciuchini, E. Franco, V. Lubicz, G. Martinelli, I. Scimemi, and L. Silvestrini, *Nucl. Phys.* **B523**, 501 (1998).
- [81] A. J. Buras, M. Misiak, and J. Urban, *Nucl. Phys.* **B586**, 397 (2000).
- [82] A. K. Alok, B. Bhattacharya, D. Kumar, J. Kumar, D. London, and S. U. Sankar, *Phys. Rev. D* **96**, 015034 (2017).
- [83] W. Altmannshofer, S. Gori, M. Pospelov, and I. Yavin, *Phys. Rev. Lett.* **113**, 091801 (2014).
- [84] A. Falkowski, S. F. King, E. Perdomo, and M. Pierre, [arXiv:1803.04430](https://arxiv.org/abs/1803.04430).
- [85] L. Di Luzio and M. Nardecchia, *Eur. Phys. J. C* **77**, 536 (2017).
- [86] L. Di Luzio, J. F. Kamenik, and M. Nardecchia, *Eur. Phys. J. C* **77**, 30 (2017).
- [87] M. Aaboud *et al.* (ATLAS Collaboration), *J. High Energy Phys.* **10**, (2017) 182.
- [88] B. C. Allanach, B. Gripaios, and T. You, *J. High Energy Phys.* **03** (2018) 021.
- [89] G. Hiller and M. Schmaltz, *Phys. Rev. D* **90**, 054014 (2014).
- [90] B. Gripaios, M. Nardecchia, and S. A. Renner, *J. High Energy Phys.* **05** (2015) 006.
- [91] I. de Medeiros Varzielas and G. Hiller, *J. High Energy Phys.* **06** (2015) 072.

- [92] D. Becirevic, S. Fajfer, and N. Kosnik, *Phys. Rev. D* **92**, 014016 (2015).
- [93] R. Alonso, B. Grinstein, and J. Martin Camalich, *J. High Energy Phys.* **10** (2015) 184.
- [94] M. Bauer and M. Neubert, *Phys. Rev. Lett.* **116**, 141802 (2016).
- [95] S. Fajfer and N. Kosnik, *Phys. Lett. B* **755**, 270 (2016).
- [96] R. Barbieri, G. Isidori, A. Pattori, and F. Senia, *Eur. Phys. J. C* **76**, 67 (2016).
- [97] D. Becirevic, N. Kosnik, O. Sumensari, and R. Zukanovich Funchal, *J. High Energy Phys.* **11** (2016) 035.
- [98] D. Becirevic, S. Fajfer, N. Kosnik, and O. Sumensari, *Phys. Rev. D* **94**, 115021 (2016).
- [99] A. Crivellin, D. Muller, and T. Ota, *J. High Energy Phys.* **09** (2017) 040.
- [100] G. Hiller and I. Nisandzic, *Phys. Rev. D* **96**, 035003 (2017).
- [101] D. Becirevic and O. Sumensari, *J. High Energy Phys.* **08** (2017) 104.
- [102] I. Dorsner, S. Fajfer, D. A. Faroughy, and N. Kosnik, *J. High Energy Phys.* **10** (2017) 188.
- [103] N. Assad, B. Fornal, and B. Grinstein, *Phys. Lett. B* **777**, 324 (2018).
- [104] L. Di Luzio, A. Greljo, and M. Nardecchia, *Phys. Rev. D* **96**, 115011 (2017).
- [105] L. Calibbi, A. Crivellin, and T. Li, [arXiv:1709.00692](https://arxiv.org/abs/1709.00692).
- [106] M. Bordone, C. Cornella, J. Fuentes-Martin, and G. Isidori, *Phys. Lett. B* **779**, 317 (2018).
- [107] S. Davidson, D. C. Bailey, and B. A. Campbell, *Z. Phys. C* **61**, 613 (1994).
- [108] I. Dorner, S. Fajfer, A. Greljo, J. F. Kamenik, and N. Konik, *Phys. Rep.* **641**, 1 (2016).
- [109] C. Biggio, M. Bordone, L. Di Luzio, and G. Ridolfi, *J. High Energy Phys.* **10** (2016) 002.
- [110] C. Bobeth and A. J. Buras, *J. High Energy Phys.* **02** (2018) 101.
- [111] A. M. Sirunyan *et al.* (CMS Collaboration), *J. High Energy Phys.* **07** (2017) 121.
- [112] J. P. Lees *et al.* (BABAR Collaboration), *Phys. Rev. D* **88**, 072012 (2013).
- [113] R. Aaij *et al.* (LHCb Collaboration), *Phys. Rev. Lett.* **115**, 111803 (2015); **115**, 159901(E) (2015).
- [114] S. Hirose *et al.* (Belle Collaboration), *Phys. Rev. Lett.* **118**, 211801 (2017).
- [115] F. Feruglio, P. Paradisi, and A. Pattori, *Phys. Rev. Lett.* **118**, 011801 (2017).
- [116] F. Feruglio, P. Paradisi, and A. Pattori, *J. High Energy Phys.* **09** (2017) 061.
- [117] D. Buttazzo, A. Greljo, G. Isidori, and D. Marzocca, *J. High Energy Phys.* **11** (2017) 044.
- [118] A. Greljo, G. Isidori, and D. Marzocca, *J. High Energy Phys.* **07** (2015) 142.
- [119] A. Lenz and U. Nierste, *J. High Energy Phys.* **06** (2007) 072.
- [120] J. Charles, A. Hocker, H. Lacker, S. Laplace, F. R. Le Diberder, J. Malcles, J. Ocariz, M. Pivk, and L. Roos (CKMfitter Group), *Eur. Phys. J. C* **41**, 1 (2005).
- [121] A. J. Buras, S. Jager, and J. Urban, *Nucl. Phys.* **B605**, 600 (2001).
- [122] C. Patrignani *et al.* (Particle Data Group), *Chin. Phys. C* **40**, 100001 (2016).
- [123] M. Beneke, A. Maier, J. Piclum, and T. Rauh, *Nucl. Phys.* **B891**, 42 (2015).
- [124] M. Beneke, A. Maier, J. Piclum, and T. Rauh, *Proc. Sci.*, RADCOR2015 (2016) 035 [[arXiv:1601.02949](https://arxiv.org/abs/1601.02949)].
- [125] M. Bona *et al.* (UTfit Collaboration), *J. High Energy Phys.* **10** (2006) 081.
- [126] F. Herren and M. Steinhauser, *Comput. Phys. Commun.* **224**, 333 (2018).
- [127] P. A. Baikov, K. G. Chetyrkin, and J. H. Khn, *Phys. Rev. Lett.* **118**, 082002 (2017).
- [128] F. Herzog, B. Ruijl, T. Ueda, J. A. M. Vermaseren, and A. Vogt, *J. High Energy Phys.* **02** (2017) 090.
- [129] T. Luthe, A. Maier, P. Marquard, and Y. Schroder, *J. High Energy Phys.* **03** (2017) 020.
- [130] T. Luthe, A. Maier, P. Marquard, and Y. Schroder, *J. High Energy Phys.* **10** (2017) 166.
- [131] K. G. Chetyrkin, G. Falcioni, F. Herzog, and J. A. M. Vermaseren, *J. High Energy Phys.* **10** (2017) 179; **12** (2017) 6.
- [132] R. J. Dowdall, C. T. H. Davies, R. R. Horgan, G. P. Lepage, C. J. Monahan, and J. Shigemitsu, [arXiv:1411.6989](https://arxiv.org/abs/1411.6989).
- [133] N. Carrasco *et al.* (ETM Collaboration), *J. High Energy Phys.* **03** (2014) 016.
- [134] E. Gamiz, C. T. H. Davies, G. P. Lepage, J. Shigemitsu, and M. Wingate (HPQCD Collaboration), *Phys. Rev. D* **80**, 014503 (2009).
- [135] S. Aoki *et al.*, *Eur. Phys. J. C* **74**, 2890 (2014).
- [136] P. Gelhausen, A. Khodjamirian, A. A. Pivovarov, and D. Rosenthal, *Phys. Rev. D* **88**, 014015 (2013); **91**, 099901(E) (2015).
- [137] E. Dalgic, A. Gray, E. Gamiz, C. T. H. Davies, G. P. Lepage, J. Shigemitsu, H. Trotter, and M. Wingate, *Phys. Rev. D* **76**, 011501 (2007).
- [138] Y. Aoki, T. Ishikawa, T. Izubuchi, C. Lehner, and A. Soni, *Phys. Rev. D* **91**, 114505 (2015).
- [139] C. M. Bouchard, E. D. Freeland, C. Bernard, A. X. El-Khadra, E. Gamiz, A. S. Kronfeld, J. Laiho, and R. S. Van de Water, *Proc. Sci.*, LATTICE2011 (2011) 274 [[arXiv:1112.5642](https://arxiv.org/abs/1112.5642)].
- [140] T. Ishikawa (private communication).
- [141] I. Caprini, L. Lellouch, and M. Neubert, *Nucl. Phys.* **B530**, 153 (1998).
- [142] C. G. Boyd, B. Grinstein, and R. F. Lebed, *Phys. Rev. Lett.* **74**, 4603 (1995).
- [143] B. Grinstein and A. Kobach, *Phys. Lett. B* **771**, 359 (2017).
- [144] D. Bigi, P. Gambino, and S. Schacht, *J. High Energy Phys.* **11** (2017) 061.
- [145] F. U. Bernlochner, Z. Ligeti, M. Papucci, and D. J. Robinson, *Phys. Rev. D* **96**, 091503 (2017).
- [146] S. Jaiswal, S. Nandi, and S. K. Patra, *J. High Energy Phys.* **12** (2017) 060.
- [147] S. Descotes-Genon (private communication), see also [148].
- [148] S. Descotes-Genon and P. Koppenburg, *Annu. Rev. Nucl. Part. Sci.* **67**, 97 (2017).